



ELSEVIER

Contents lists available at ScienceDirect

## Journal of Magnetism and Magnetic Materials

journal homepage: [www.elsevier.com/locate/jmmm](http://www.elsevier.com/locate/jmmm)The normal and inverse magnetocaloric effect in  $\text{RCu}_2$  (R=Tb, Dy, Ho, Er) compoundsX.Q. Zheng<sup>a,\*</sup>, Z.Y. Xu<sup>b</sup>, B. Zhang<sup>c</sup>, F.X. Hu<sup>c</sup>, B.G. Shen<sup>c,\*</sup><sup>a</sup> School of Materials Science and Engineering, University of Science and Technology Beijing, Beijing 100083, People's Republic of China<sup>b</sup> National Institute of Metrology, Beijing 100029, People's Republic of China<sup>c</sup> State Key Laboratory for Magnetism, Institute of Physics, Chinese Academy of Sciences, Beijing 100190, People's Republic of China

## ARTICLE INFO

## Article history:

Received 15 July 2016

Received in revised form

14 August 2016

Accepted 15 August 2016

Available online 16 August 2016

## Keywords:

Magnetocaloric effect

Magnetic materials

Magnetic entropy change

## ABSTRACT

Orthorhombic polycrystalline  $\text{RCu}_2$  (R=Tb, Dy, Ho and Er) compounds were synthesized and the magnetic properties and magnetocaloric effect (MCE) were investigated in detail. All of the  $\text{RCu}_2$  compounds are antiferromagnetic (AFM) ordered. As temperature increases,  $\text{RCu}_2$  compounds undergo an AFM to AFM transition at  $T_i$  and an AFM to paramagnetic (PM) transition at  $T_N$ . Besides of the normal MCE around  $T_N$ , large inverse MCE around  $T_i$  was found in  $\text{TbCu}_2$  compound. Under a field change of 0–7 T, the maximal value of inverse MCE is even larger than the value of normal MCE around  $T_N$  for  $\text{TbCu}_2$  compound. Considering of the normal and inverse MCE,  $\text{TbCu}_2$  shows the largest refrigerant capacity among the  $\text{RCu}_2$  (R=Tb, Dy, Ho and Er) compounds indicating its potential applications in low temperature multistage refrigeration.

© 2016 Elsevier B.V. All rights reserved.

## 1. Introduction

Magnetocaloric effect (MCE) is the intrinsic property of magnetic materials and the magnetic refrigeration based on MCE has been demonstrated as a promising alternative to the conventional gas compression or expansion refrigeration for its high energy efficiency and environmental friendliness [1–3]. Lots of efforts were made to explore the room-temperature MCE materials such as  $\text{Gd}_5\text{Si}_2\text{Ge}_2$  [4],  $\text{La}(\text{Fe}, \text{Si})_{13}$  [5–8],  $\text{MnAs}_{1-x}\text{Sb}_x$  [9],  $\text{MnFeP}_{1-x}\text{As}_x$  [10],  $\text{NiMnSn}$  [11],  $\text{NiMnIn}$  [12], etc. In the past few years, much attention has also been paid on the MCE materials with low transition temperatures such as  $\text{ErCo}_2$  [13],  $\text{HoCuAl}$  [14],  $\text{PrSi}$  [15],  $\text{RAI}_2$  [16,17] and so on, because these materials are promising to be used for gas liquefaction in magnetic cooling cycle or combined magnetic-gas cooling cycle [18,19]. Most of the low temperature MCE materials have been summarized in the review papers [20,21]. The isothermal magnetic entropy change ( $\Delta S_M$ ) is one of the important parameters to evaluate MCE materials. For most MCE materials, the value of  $\Delta S_M$  is negative, which can also be described as normal MCE. The positive  $\Delta S_M$  can also be observed and it has been stated as inverse MCE [11]. The inverse MCE has been observed in Heusler alloys such as  $\text{NiMnSn}$  [11] and some antiferromagnetic (AFM) materials such as  $\text{DySb}$  [22], and  $\text{ErRu}_2\text{Si}_2$

[23]. However, in most AFM materials the inverse MCE can only be observed under low magnetic field change and the value of positive magnetic entropy change is not large.

Rare earth (R) based intermetallic compounds have shown interesting magnetic properties and excellent performance on MCE. Orthorhombic  $\text{RCu}_2$  series is one of the important categories of R-based intermetallic compounds and the magnetic properties of single crystal and polycrystalline  $\text{RCu}_2$  (R=Ce–Lu) compounds have been investigated in detail [24–29]. Results show that the ground state of most  $\text{RCu}_2$  compounds is AFM and the field-induced metamagnetic transition was observed. Much work has also been done on the specific heat, magnetoresistance, magnetostriction in  $\text{RCu}_2$  compounds [30–35]. Giant magnetostriction was observed in  $\text{TbCu}_2$  and  $\text{DyCu}_2$  crystals. The magnetic structures and magnetic transitions of  $\text{HoCu}_2$  compound were investigated by magnetic, specific heat and Neutron Powder Diffraction experiments [36–38]. Two magnetic transitions were observed in  $\text{HoCu}_2$  compound at 7.4 K and 10.5 K, respectively [33,36,37]. The lower transition temperature was corresponding to AFM to AFM transition and the higher temperature was corresponding to AFM to paramagnetic (PM) transition. The MCE of  $\text{HoCu}_2$  and  $\text{DyCu}_2$  compounds have also been studied. An effective refrigerant capacity of 194 J/kg below 44 K was obtained in  $\text{DyCu}_2$  compound, and a maximum  $\Delta S_M$  of 19.3 J/kg K with a relative cooling power of 268 J/kg was found in  $\text{HoCu}_2$  compound [39,40].

Considering of the interesting magnetic properties of  $\text{RCu}_2$  compounds, further study on MCE will be performed. In this work, the  $\text{RCu}_2$  (R=Tb, Dy, Ho, Er) compounds were synthesized

\* Corresponding authors.

E-mail addresses: [zhengxq@ustb.edu.cn](mailto:zhengxq@ustb.edu.cn) (X.Q. Zheng), [shenbg@aphy.iphy.ac.cn](mailto:shenbg@aphy.iphy.ac.cn) (B.G. Shen).

successfully. The magnetic properties and magnetocaloric effect were investigated in detail. Especially, the normal and inverse MCEs in  $\text{RCu}_2$  compounds were analyzed and discussed.

## 2. Experimental procedure

Polycrystalline  $\text{RCu}_2$  ( $\text{R}=\text{Tb}, \text{Dy}, \text{Ho}, \text{Er}$ ) compounds were prepared by arc-melting method with a high-purity argon atmosphere. The purities of starting materials were better than 99.9%. The ingots were turned over and remelted several times to ensure their homogeneity. After arc-melting, the samples were subsequently wrapped by molybdenum foil, sealed in a high-vacuum quartz tube, annealed at 700 °C for 7 days and finally quenched to liquid nitrogen. The crystal structure was characterized by powder X-ray diffraction (XRD) method with  $\text{Cu K}\alpha$  radiation. Magnetic measurements (including  $M$ - $T$  and  $M$ - $H$  curves) were performed by employing Vibrating Sample Magnetometer with Quantum Design (SQUID-VSM).

## 3. Results and discussion

The XRD patterns of  $\text{RCu}_2$  ( $\text{R}=\text{Tb}, \text{Dy}, \text{Ho}, \text{Er}$ ) compounds at room temperature are shown in Fig. 1. Almost all of the diffraction peaks can be indexed to an orthorhombic crystal structure (space group  $Imma$  #74). The result is in accord with previous work [38]. The Bragg positions are marked at the bottom of the picture. It can also be seen that there is a small impure peak around 31.7° for  $\text{ErCu}_2$  compound, which indicates that small amount of impurity may exist. However, it does not affect the discussion in the following section because the amount of purity is not large. That is to say, almost all the obtained  $\text{RCu}_2$  ( $\text{R}=\text{Tb}, \text{Dy}, \text{Ho}, \text{Er}$ ) compounds are synthesized successfully. The lattice parameters were determined by using Rietveld refinement method. For example, the lattice constant of  $\text{HoCu}_2$  compound is calculated as follows:  $a=4.2871(2)$  Å,  $b=6.7777(4)$  Å and  $c=7.2761(0)$  Å. As the atom number of R increases, the position of diffraction peak moves towards higher angle range. It indicates that the lattice constant becomes smaller and smaller from  $\text{TbCu}_2$  to  $\text{ErCu}_2$  compound. Results show that the  $\text{RCu}_2$  compounds crystallize in orthorhombic  $\text{CeCu}_2$ -type structure, which can be considered as a stacking of alternating layers of R and Cu atoms along  $c$  axis of crystal [38].

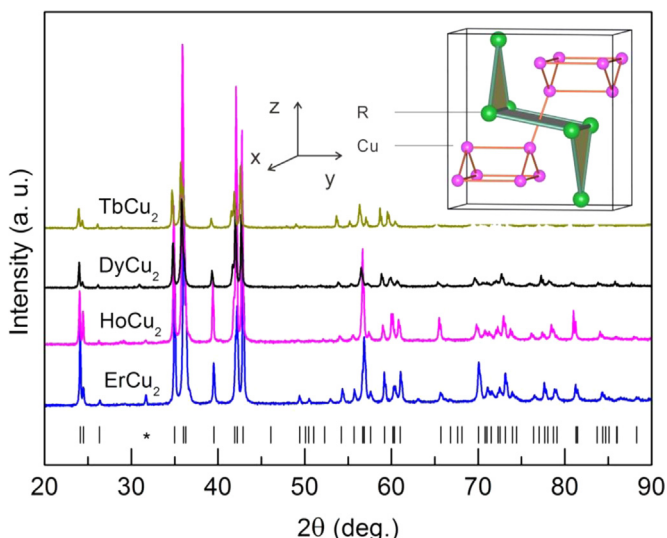
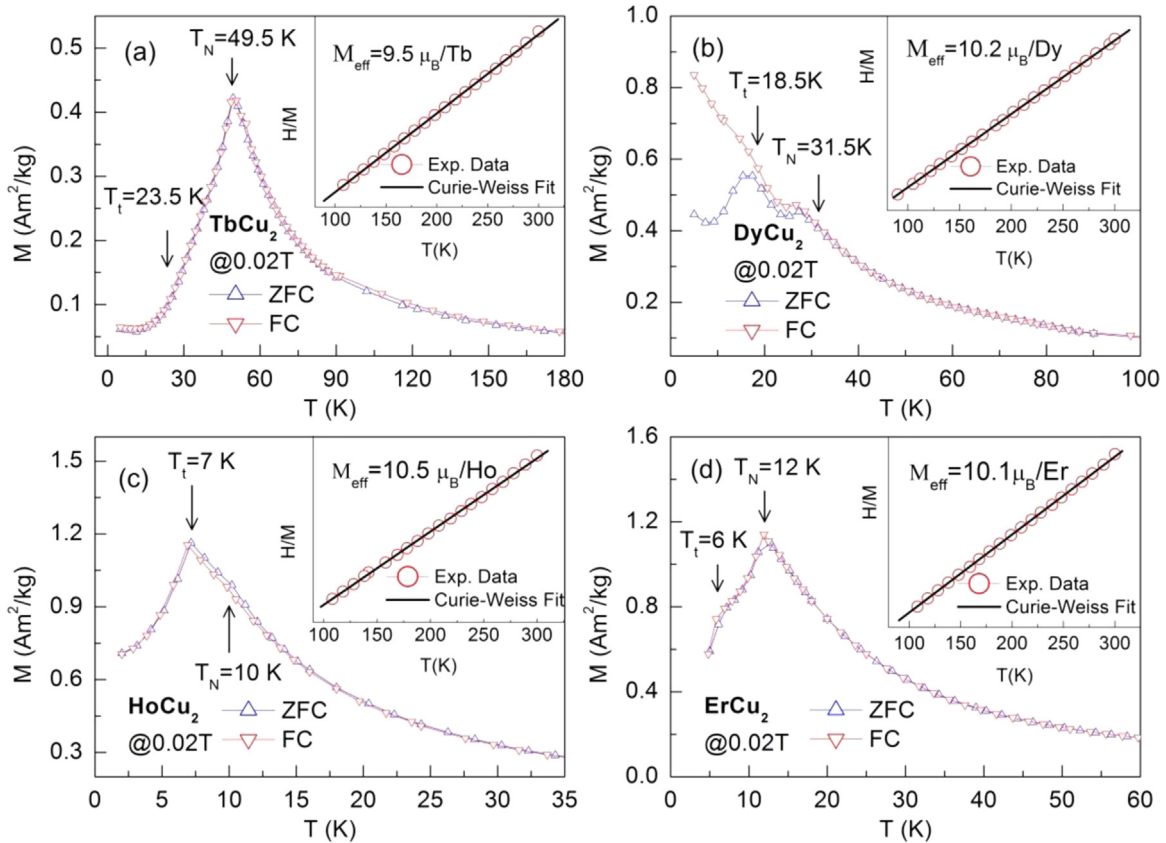


Fig. 1. The XRD patterns of  $\text{RCu}_2$  ( $\text{R}=\text{Tb}, \text{Dy}, \text{Ho}$  and  $\text{Er}$ ) compounds measured at room temperature. Inset: the crystal structure of  $\text{RCu}_2$  in one unit cell.

The crystal structure of  $\text{RCu}_2$  compounds is shown in the inset of Fig. 1. It can be seen that there are four R atoms in form of one parallelepiped along with two triangles and eight Cu atoms in form of two triangular prisms in the unit cell.

The Zero-Field-Cooled (ZFC) and Field-Cooled (FC) magnetization curves were measured at a field of 0.02 T for  $\text{RCu}_2$  ( $\text{R}=\text{Tb}, \text{Dy}, \text{Ho}, \text{Er}$ ) compounds and they are shown in Fig. 2(a)–(d), respectively. The magnetization of  $\text{TbCu}_2$  compound shows a fixed and small value at low temperatures, increases rapidly at higher temperatures and then goes down quickly with temperature increasing further. The two drastic changes correspond to two magnetic phase transitions: antiferromagnetic (AFM) to AFM transition and an AFM to paramagnetic (PM) transition. The transition temperatures were determined to be  $T_t=23.5$  K and  $T_N=49.5$  K, respectively. The other  $\text{RCu}_2$  ( $\text{R}=\text{Dy}, \text{Ho}, \text{Er}$ ) compounds were also observed to experience the same two magnetic phase transitions. As for  $\text{HoCu}_2$  compound, the thermal magnetization curves corresponding to AFM to AFM transition shows a more drastic change than that corresponding to AFM to PM transition does. That the order-order magnetic transition is more obvious than order-disorder magnetic transition has been reported in other R-based compound such as  $\text{PrGa}$  [41]. In fact, the two magnetic transitions for  $\text{HoCu}_2$  compound have been confirmed according to neutron powder diffraction and specific heat experiments [33,36,37]. The determined transition temperatures in this work are in good accordance with the reported temperatures. The effective magnetic moments have also been calculated according to the Curie-Weiss Law fitting of  $M$ - $T$  curves in high temperature range. The fitting lines are shown in the inset of Fig. 2(a)–(d). All the transition temperatures, effective magnetic moments and ion magnetic moments for  $\text{RCu}_2$  ( $\text{R}=\text{Tb}, \text{Dy}, \text{Ho}, \text{Er}$ ) compounds are shown in Table 1. As the atomic number increases, the value of  $T_t$  shows a decrease trend. The value of  $T_N$  also shows a decrease trend in general, but there is an exception in  $\text{ErCu}_2$ . It may be correlated to the complex magnetic coupling in  $\text{ErCu}_2$  compound. According to the comparison of effective moments and ion moments for each compound, the value is almost the same for each compound, which indicates only Rare earth atoms contribute to the magnetic moments in  $\text{RCu}_2$  ( $\text{R}=\text{Tb}, \text{Dy}, \text{Ho}, \text{Er}$ ) compounds.

For most magnetic materials, magnetocaloric effect (MCE) can be observed around transition temperatures. In general, the performance of MCE materials is evaluated by isothermal magnetic entropy change ( $\Delta S_M$ ). For magnetic materials, the total entropy can be written as:  $S=S_E+S_L+S_M$ . In the above expression,  $S$  is the total entropy, and  $S_E$ ,  $S_L$  and  $S_M$  are the entropy contributed by electrons, lattice and magnetic moments, respectively. For the second order transition system, external magnetic field usually affect  $S_M$  only, and then  $\Delta S$  equals  $\Delta S_M$ . It should be mentioned that for the case of first order transition systems, the  $S_L$  is more significant. Under the situation that temperature and magnetic field are the only two variables, the differential forms of  $S$  can be written as:  $dS=\frac{\partial S}{\partial T}dT+\frac{\partial S}{\partial H}dH$ . Considering of the definition of entropy and Maxwell relationship ( $\frac{\partial S}{\partial T}=\frac{C}{T}$ ,  $\frac{\partial S}{\partial H}=\frac{\partial M}{\partial T}$ ), the above expression can be written as:  $dS=\frac{C}{T}dT+\frac{\partial M}{\partial T}dH$ . Under the isothermal condition, magnetic entropy change can be calculated as:  $\Delta S_M=\int_0^H\left(\frac{\partial M}{\partial T}\right)dH$ . The temperature dependences of  $\Delta S_M$  under a field change of 0–2 T, 0–5 T and 0–7 T for  $\text{RCu}_2$  ( $\text{R}=\text{Tb}, \text{Dy}, \text{Ho}, \text{Er}$ ) compounds are shown in Fig. 3(a)–(d), respectively. Since the value of  $(dM/dT)$  is negative around  $T_N$ , the value of  $\Delta S_M$  is negative as well. And the presented plots are  $-\Delta S_M$  versus  $T$  curves. It can be clearly seen that there is a large peak around  $T_N$  for all the  $\text{RCu}_2$  compounds. The negative  $\Delta S_M$  around  $T_N$  is so called normal MCE. RC is calculated by using the approach  $\text{RC}=\int_{T_L}^{T_H}|\Delta S_M|dT$ , where  $T_L$  and  $T_H$  are the temperatures corresponding to the full width at half



**Fig. 2.** The ZFC and FC curves of  $RCu_2$  ( $R = \text{Tb, Dy, Ho}$  and  $\text{Er}$ ) compounds at a field of 0.02 T. Inset: temperature dependence curve of  $\chi^{-1}$  and the fitting, where  $\chi$  is the magnetic susceptibility. (a)  $\text{TbCu}_2$ . (b)  $\text{DyCu}_2$ . (c)  $\text{HoCu}_2$ . (d)  $\text{ErCu}_2$ .

**Table 1**

The transition temperatures, effective magnetic moments, ion magnetic moments, MCE parameters of  $RCu_2$  ( $R = \text{Tb, Dy, Ho}$  and  $\text{Er}$ ) compounds.

	$T_i$ (K)	$T_N$ (K)	$M_{\text{eff}}$ ( $\mu_B$ )	$M_{\text{ion}}$ ( $\mu_B$ )	MCE_0–5 T			MCE_0–7 T		
					$-\Delta S_M(T)_{\text{max}}$ (J/kg K)	$\delta T_{\text{FWHM}}$ (K)	RC (J/kg)	$-\Delta S_M(T)_{\text{max}}$ (J/kg K)	$\delta T_{\text{FWHM}}$ (K)	RC (J/kg)
<b>TbCu<sub>2</sub></b>	23.5	49.5	9.5	9.7	8.3	30.1	187.1	11.5	39.2	339.0
<b>TbCu<sub>2</sub>*</b>	–	–	–	–	–	–	266.4	–	–	450.7
<b>DyCu<sub>2</sub></b>	18.5	31.5	10.2	10.5	10.1	26.2	198.6	14.8	33.0	365.0
<b>HoCu<sub>2</sub></b>	7.0	10.0	10.5	10.6	15.8	16.0	194.7	21.5	20.1	330.0
<b>ErCu<sub>2</sub></b>	6.0	12.0	10.1	9.6	11.2	17.7	147.4	13.7	21.8	226.5

\* The value is revised by considering of normal and inverse MCE.

maximal  $(\Delta S_M)_{\text{max}}$ , respectively [42]. Based on the main peak (also the normal MCE), the maximal magnetic entropy change  $(-\Delta S_M)_{\text{max}}$ , refrigerant temperature width ( $\delta T_{\text{FWHM}} = T_H - T_L$ ) and refrigerant capacity (RC) have been calculated and shown in Table 1. It is found that the  $|(\Delta S_M)_{\text{max}}|$  of  $\text{HoCu}_2$  (15.8 J/kg K for 0–5 T; 21.5 J/kg K for 0–7 T) is the largest and the  $\delta T_{\text{FWHM}}$  of  $\text{HoCu}_2$  (16.0 K for 0–5 T; 20.1 K for 0–7 T) is the smallest. According to model proposed by Oesterreicher et al. [43],  $|(\Delta S_M)_{\text{max}}|$  is negatively correlated with  $T_C$  or  $T_N$  and positively correlated with total angular momentum quantum number ( $J$ ). As for  $RCu_2$  compounds,  $\text{HoCu}_2$  shows the smallest  $T_N$  and the largest  $J$ , thus  $\text{HoCu}_2$  shows the largest  $|(\Delta S_M)_{\text{max}}|$ . It is found that  $\text{DyCu}_2$  compound shows the largest value of RC among the  $RCu_2$  compounds. The value of RC in  $\text{DyCu}_2$  compound is calculated to be 198.6 J/kg and 365.0 J/kg for a field change of 0–5 T and 0–7 T, respectively.

According to the characteristic of  $M$ – $T$  curves, the value of  $(dM/dT)$  is positive in low temperature range for the  $RCu_2$  compounds. As a result, positive  $\Delta S_M$  was observed around  $T_i$  for all the  $RCu_2$  compounds, which is the so-called inverse MCE. For  $\text{HoCu}_2$  and

$\text{ErCu}_2$  compounds, the positive  $\Delta S_M$  can only be observed under a very low field change, for example, under a field change of 0–1 T (the inset of Fig. 3(c) and (d)). When the field change is larger than 2 T, the positive  $\Delta S_M$  disappears, which indicates that the AFM ground state in low temperature range is weak. As for  $\text{DyCu}_2$ , the positive  $\Delta S_M$  can be kept even the field change is as high as 0–2 T, which means the AFM ground state is stronger than that in  $\text{HoCu}_2$  and  $\text{ErCu}_2$ . In fact, inverse MCE has been observed in many Heusler alloys and AFM magnetocaloric effect materials [11,23]. The cause of positive  $\Delta S_M$  results from the mixed exchange interaction and the applied magnetic field leads to a further spin-disordered state [11]. In the reported AFM materials, the positive  $\Delta S_M$  at low temperatures is usually far smaller than the absolute value of negative  $\Delta S_M$  near  $T_N$  and it disappears when the field change becomes larger, which is the same as the case in  $\text{HoCu}_2$  and  $\text{ErCu}_2$ . But incredible results were found in  $\text{TbCu}_2$  compound. Firstly, the inverse MCE is kept at a high field change such as 0–7 T, which indicates the magnetic moments are in strong AFM order in  $\text{TbCu}_2$  compound. Secondly, the maximal positive  $\Delta S_M$  (13.9 J/kg K) is

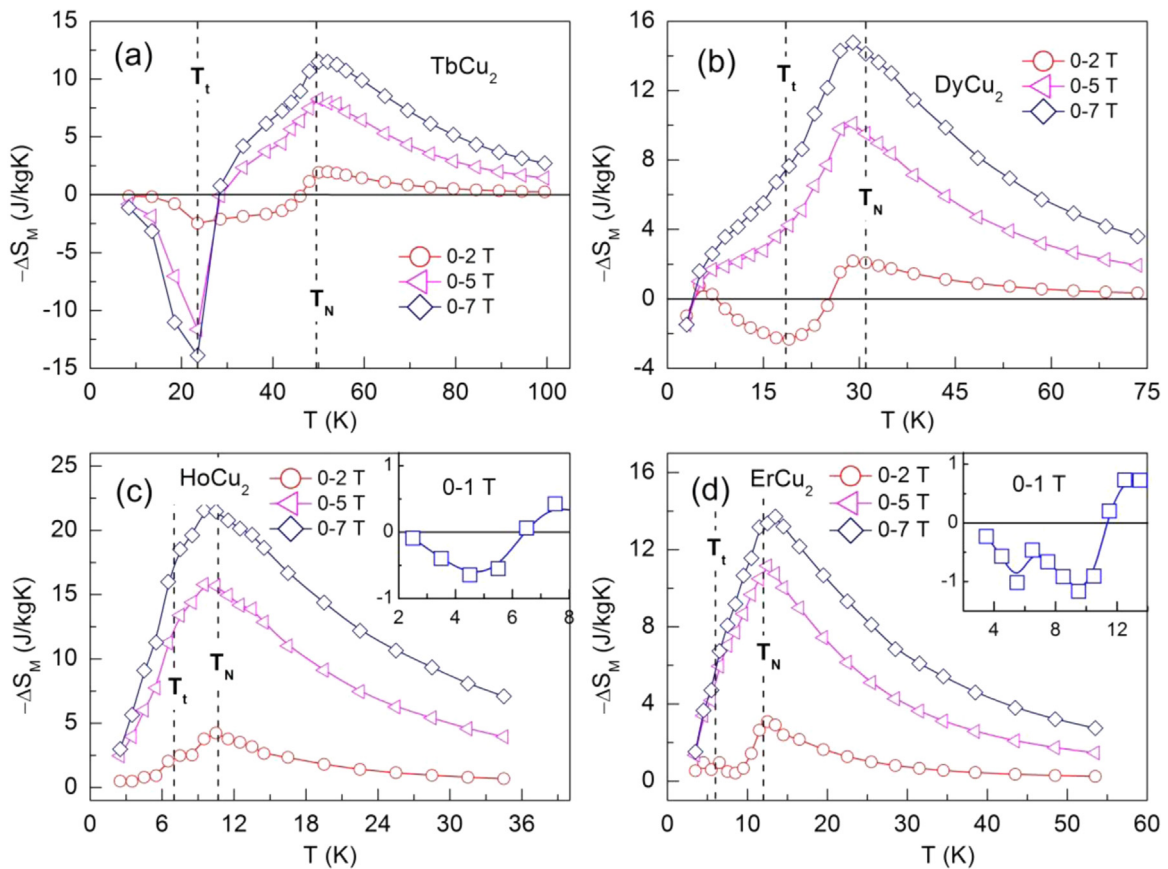


**Fig. 3.** The temperature dependences of  $\Delta S_M$  at a field change of 0–2 T, 0–5 T and 0–7 T for  $RCu_2$  ( $R = \text{Tb, Dy, Ho}$  and  $\text{Er}$ ) compounds, respectively. Inset: the  $\Delta S_M$  curve in low temperature range at a field change of 0–1 T. (a)  $\text{TbCu}_2$ . (b)  $\text{DyCu}_2$ . (c)  $\text{HoCu}_2$ . (d)  $\text{ErCu}_2$ .

larger than the maximal value around  $T_N$  (11.5 J/kg K), and the above results are rarely seen in other AFM MCE materials. It can be seen that  $\text{DyCu}_2$  and  $\text{TbCu}_2$  compounds show much larger inverse magnetocaloric effect compared with  $\text{HoCu}_2$  and  $\text{ErCu}_2$  compounds. It results from the strong AFM coupling in  $\text{DyCu}_2$  and  $\text{TbCu}_2$  compounds. The strong AFM order may be related to the large magnetocrystalline anisotropy of Dy and Tb atoms. The inverse MCE can also be used for magnetic refrigeration if only the refrigerator works in a reverse process. For  $\text{TbCu}_2$  compound, magnetic refrigeration can be realized in a usual working recycle above 30 K and it can be used in a reverse working recycle below 30 K. That is to say,  $\text{TbCu}_2$  compound is very useful in multistage refrigeration. In order to evaluate  $\text{TbCu}_2$  more comprehensively, the RC of  $\text{TbCu}_2$  compound is re-calculated by considering of the contribution of inverse MCE at lower temperatures. The updated value of RC including normal MCE and inverse MCE is also shown in Table 1 for  $\text{TbCu}_2$  compound. The modified value of RC for a field change of 0–5 T and 0–7 T is 266.4 J/kg and 450.7 J/kg, respectively. It is found that  $\text{TbCu}_2$  compound shows the largest RC among the  $RCu_2$  compounds. The excellent performance of  $\text{TbCu}_2$  compound indicates its potential applications in low temperature refrigeration.

#### 4. Conclusion

In summary, orthorhombic polycrystalline  $RCu_2$  ( $R = \text{Tb, Dy, Ho}$  and  $\text{Er}$ ) compounds were fabricated and the magnetic properties were investigated in detail. Results show that  $RCu_2$  ( $R = \text{Tb, Dy, Ho}$  and  $\text{Er}$ ) compounds are AFM ordered and all of them undergo two magnetic phase transitions: an AFM to AFM transition at  $T_t$  and an

AFM to PM transition at  $T_N$ . The AFM ground state is so strong that inverse MCE was observed even under a large field change for  $\text{TbCu}_2$  compound. Considering of the normal and inverse MCE,  $\text{TbCu}_2$  compound shows the largest RC among the  $RCu_2$  ( $R = \text{Tb, Dy, Ho}$  and  $\text{Er}$ ) compounds, indicating its potential applications in the magnetic refrigeration in the future.

#### Acknowledgment

This work was supported by the National Natural Science Foundation of China (Nos. 51501005, 11274357, 51531008 and 51271196), the Fundamental Research Funds for the Central Universities (No. FRF-TP-15-010A1) and the China Postdoctoral Science Foundation funded project (2016M591071).

#### References

- [1] E. Brück, *J. Phys. D Appl. Phys.* 38 (2005) R381–R391.
- [2] V.K. Pecharsky, K.A. Gschneidner Jr., *J. Magn. Magn. Mater.* 200 (1999) 44–56.
- [3] K.A. Gschneidner Jr., V.K. Pecharsky, *Annu. Rev. Matter Sci.* 30 (2000) 387–429.
- [4] V.K. Pecharsky, K.A. Gschneidner, *Phys. Rev. Lett.* 78 (1997) 4494–4497.
- [5] F.X. Hu, B.G. Shen, J.R. Sun, Z.H. Cheng, G.H. Rao, X.X. Zhang, *Appl. Phys. Lett.* 78 (2001) 3675–3677.
- [6] F.X. Hu, B.G. Shen, J.R. Sun, X.X. Zhang, *Chin. Phys.* 9 (2000) 0550–0553.
- [7] X.X. Zhang, G.H. Wen, F.W. Wang, W.H. Wang, C.H. Yu, G.H. Wu, *Appl. Phys. Lett.* 77 (2000) 3072–3074.
- [8] X.X. Zhang, F.W. Wang, G.H. Wen, *J. Phys.: Condens. Matter* 13 (2001) L747–L752.
- [9] H. Wada, Y. Tanabe, *Appl. Phys. Lett.* 79 (2001) 3302–3304.
- [10] O. Tegus, E. Brück, K.H.J. Buschow, F.R. de Boer, *Nature* 415 (2002) 150–152.
- [11] T. Krenke, E. Duman, M. Acet, E.F. Wassermann, X. Moya, L. Mañosa, A. Planes, *Nat. Mater.* 4 (2005) 450–454.
- [12] J. Liu, T. Gottschall, K.P. Skokov, J.D. Moore, O. Gutfleisch, *Nat. Mater.* 11 (2012)



- 620–626.
- [13] A. Giguere, M. Foldeaki, W. Schnelle, E. Gmelin, *J. Phys.: Condens. Matter* 11 (1999) 6969–6981.
- [14] Q.Y. Dong, J. Chen, J. Shen, J.R. Sun, B.G. Shen, *J. Magn. Magn. Mater.* 324 (2012) 2676–2678.
- [15] L.C. Wang, B.G. Shen, *Rare Met.* 33 (2014) 239–243.
- [16] F.W. Wang, X.X. Zhang, F.X. Hu, *Appl. Phys. Lett.* 77 (2000) 1360–1362.
- [17] M. Khan, K.A. Gschneidner, V.K. Pecharsky, *J. Magn. Magn. Mater.* 324 (2012) 1381–1384.
- [18] H. Yayama, Y. Hatta, Y. Makimoto, A. Tomokiyo, *Jpn. J. Appl. Phys.* 39 (2000) 4220–4224.
- [19] K.A. Gschneidner Jr., V.K. Pecharsky, A.O. Tsokol, *Rep. Prog. Phys.* 68 (2005) 1479–1539.
- [20] H. Zhang, B.G. Shen, *Chin. Phys. B* 24 (2015) 127504.
- [21] L.W. Li, *Chin. Phys. B* 25 (2016) 037502.
- [22] W.J. Hu, J. Du, B. Li, Q. Zhang, Z.D. Zhang, *Appl. Phys. Lett.* 92 (2008) 192505.
- [23] T. Samanta, I. Das, S. Banerjee, *Appl. Phys. Lett.* 91 (2007) 152506.
- [24] R.C. Sherwood, H.J. Williams, J.H. Wernick, *J. Appl. Phys.* 35 (1964) 1049.
- [25] Y. Hashimoto, H. Fujii, T. Okamoto, *J. Phys. Soc. Jpn.* 40 (1976) 1519–1520.
- [26] K. Sugiyama, M. Nakashima, Y. Yoshida, R. Settai, T. Takeuchi, K. Kindo, Y. Onuki, *Physica B* 259 (1996) 896.
- [27] R. Settai, P. Ahmet, K. Araki, M. Abliz, K. Sugiyama, Y. Onuki, *Physica B* 230 (1997) 766.
- [28] M. Loewenhaupt, M. Doerr, L. Jahn, T. Reif, C. Sierks, M. Rotter, H. Muller, *Physica B* 246 (1998) 472.
- [29] Y. Yoshida, K. Sugiyama, T. Takeuchi, Y. Kimura, D. Aoki, M. Kouzaki, R. Settai, K. Kindo, Y. Onuki, *J. Phys. Soc. Jpn.* 67 (1998) 1421–1430.
- [30] R.R. Birss, R.V. Houldsworth, D.G. Lord, *J. Magn. Magn. Mater.* 15 (1980) 917–918.
- [31] E. Gratz, V. Sechovsky, V. Sima, Z. Smetana, J.O. Ström-Olson, *Phys. Status Solidi B* 111 (1982) 195–201.
- [32] N.H. Luong, J.J.M. Franse, T.D. Hien, *J. Magn. Magn. Mater.* 50 (1985) 153–160.
- [33] J. Bischof, M. Diviš, P. Svoboda, Z. Smetana, *Phys. Status Solidi A* 114 (1989) K229–K231.
- [34] M. Dorr, M. Loewenhaupt, W. Hahn, E. Brück, I.H. Hagemus, J.C.P. Klaasse, M. Rotter, *Physica B* 262 (1999) 340.
- [35] M. Doerr, M. Rotter, M. Loewenhaupt, T. Reif, P. Svoboda, *Physica B* 284 (2000) 1331.
- [36] D.G. Lord, K.A. McEwen, *J. Magn. Magn. Mater.* 15 (1980) 523–524.
- [37] Z. Smetana, V. Šíma, B. Lebech, *J. Magn. Magn. Mater.* 59 (1986) 145–152.
- [38] B. Lebech, Z. Smetana, V. Šíma, *J. Magn. Magn. Mater.* 70 (1987) 97.
- [39] P. Arora, P. Tiwari, V.G. Sathe, M.K. Chattopadhyay, *J. Magn. Magn. Mater.* 321 (2009) 3278.
- [40] S.K. Karmakar, S. Giri, S. Majumdar, *J. Appl. Phys.* 117 (2015) 193904.
- [41] X.Q. Zheng, H. Wu, J. Chen, B. Zhang, Y.Q. Li, F.X. Hu, J.R. Sun, Q.Z. Huang, B. G. Shen, *Sci. Rep.* 5 (2015) 14970.
- [42] K.A. Gschneidner Jr., V.K. Pecharsky, A.O. Pecharsky, C.B. Zimm, *Mater. Sci. Forum* 315–317 (1999) 69–76.
- [43] H. Oesterreicher, F.T. Parker, *J. Appl. Phys.* 55 (1984) 4334–4338.